

Temperature dependence of hole spin coherence in (In,Ga)As quantum dots measured by mode-locking and echo techniques

S. Varwig,¹ A. René,¹ A. Greulich,¹ D. R. Yakovlev,^{1,2} D. Reuter,³ A. D. Wieck,³ and M. Bayer¹

¹*Experimentelle Physik 2, Technische Universität Dortmund, 44221 Dortmund, Germany*

²*Ioffe Physical-Technical Institute, Russian Academy of Sciences, 194021 St. Petersburg, Russia*

³*Angewandte Festkörperphysik, Ruhr-Universität Bochum, 44780 Bochum, Germany*

(Received 17 January 2013; revised manuscript received 19 February 2013; published 13 March 2013)

The temperature dependence of the coherence time of hole spins confined in self-assembled (In,Ga)As/GaAs quantum dots is studied by spin-mode-locking and spin-echo techniques. Coherence times limited to about a microsecond are measured for temperatures below 8 K. For higher temperatures, a fast drop occurs down to a few nanoseconds over a 10-K range. The hole-nuclear hyperfine interaction appears too weak to account for these limitations. We suggest that spin-orbit-related interactions are the decisive sources for hole spin decoherence.

DOI: [10.1103/PhysRevB.87.115307](https://doi.org/10.1103/PhysRevB.87.115307)

PACS number(s): 71.70.Ej, 76.60.Lz, 78.47.jm, 78.67.Hc

During recent years, the spins of holes confined in III-V semiconductor quantum dots (QDs) have attracted considerable interest. This interest is related to the hole spin's hyperfine coupling to nuclear spins, which has been found to be non-negligible, in contrast to original suggestions based on the vanishing contact interaction, but still considerably reduced by an order of magnitude as compared to electron spins.¹⁻³ For the electrons, the hyperfine interaction has been identified as the source of spin decoherence at cryogenic temperatures.^{4,5} The transverse spin-relaxation time is on the order of microseconds at these conditions,^{6,7} well below the longitudinal spin-relaxation times of up to milliseconds in magnetic fields large enough for sizable two-level splittings that might be of use in quantum information.

From their reduced hyperfine coupling, longer coherence times may be expected for hole spins.⁸ However, recent studies have demonstrated that the hole spin-coherence time T_2 is *not* elongated, but rather, is comparable to that of the electron with values on the order of a microsecond.^{3,9,10} These times are supported by the correlation times of spin fluctuations measured through spin-noise spectroscopy in the range of a few hundred nanoseconds.^{11,12} The origin of this behavior is not yet understood: Spin-orbit interaction as another potential spin-relaxation mechanism involving phonons may be more important for holes than for electrons, but at liquid-helium temperatures, it should be suppressed in quantum dots with a discrete energy-level structure. To obtain more insight into the problem, it might be helpful to study the temperature dependence of the hole spin-coherence time.

This is the problem that we address here by exploiting the recently demonstrated hole spin mode locking (SML) in consequence of periodic pulsed excitation of the ground-state transition by circularly polarized laser light.³ By monitoring the SML signal amplitude in dependence on the laser-pulse separation at various temperatures, we find that the hole spin-coherence time remains constant in the microsecond range only up to about 8 K but then drops quickly down to nanoseconds at 20 K, approaching the lifetime of optically excited electron-hole pairs. This result is confirmed by detecting the temperature dependence of optically induced hole spin echoes. From this, we conclude that spin-orbit interactions

play the decisive role, even though details of the mechanism need further elaboration.

The sample under study was grown by molecular-beam epitaxy on a (001) GaAs substrate and contains ten layers of (In,Ga)As dots, separated by 100-nm GaAs barriers. The QD density per layer is about 10^{10} cm⁻². The dots are nominally undoped, but, in earlier studies, it was found that about half of them are singly positively charged due to residual carbon impurities.³ The sample was annealed for 30 s at a temperature of 960 °C, leading to a band-gap increase such that resonant excitation by a Ti:sapphire laser is possible. The photoluminescence (PL) spectrum in Fig. 1(a) shows the ground-state emission with a maximum at 1.38 eV and a full width at half maximum (FWHM) of about 20 meV.

To study the QD spin dynamics, we use a degenerate pump-probe setup with the laser energies tuned to the PL maximum. The optical axis (z axis) is chosen parallel to the sample growth direction. Spin polarization of the QD hole is generated by a periodic train of circularly polarized pump pulses exciting the transition from the resident hole to the positively charged exciton. The spin polarization along the z axis is monitored by measuring the ellipticity of an originally linearly polarized probe beam after transmission through the sample, which is mounted in a cryostat allowing variable temperatures T down to 2 K and magnetic fields B up to 7 T. Application of such an external magnetic field along the x axis (Voigt geometry) leads to precessions of the hole spins about this axis.

Pump and probe pulses are taken from a Ti:sapphire laser operating at a repetition frequency of 75.75 MHz, corresponding to a pulse separation of $T_R = 13.2$ ns that can be extended by a pulse picker. The pulses with durations of 1.5 ps have spectral widths of 1 meV so that an ensemble of about 10^5 QDs is addressed. The pump pulse intensity is adjusted to a pulse area of π ; the probe pulse intensity is taken five times weaker. By varying the delay between pump and probe pulses, the temporal evolution of the spin polarization is measured as shown in Fig. 1(b).

After pump incidence at zero delay, one sees damped oscillations with contributions from resident and photocreated electron and hole spins. These contributions are distinguishable by their precession frequencies due to different g factors, namely, $|g_e| = 0.58$ for electrons and $|g_h| = 0.14$ for holes.¹³

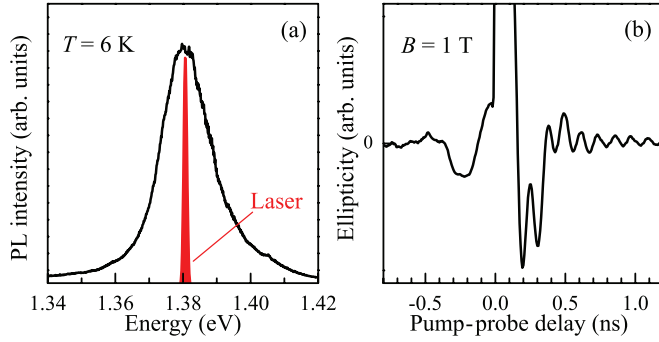


FIG. 1. (Color online) (a) Photoluminescence spectrum of the (In,Ga)As/GaAs QD ensemble, measured at $T = 6$ K. The red-colored line shows the laser spectrum with a FWHM of 1 meV, which is in resonance with the QD ground-state emission. (b) Pump-probe ellipticity measurement at $B = 1$ T and $T = 6$ K. The zero delay peak influenced by scattered laser light is cut off for better visibility of the spin-precession oscillations.

The damping of the signal arises from spin dephasing due to g -factor variations in the ensemble. In Ref. 14, we have shown that, for the in-plane hole g factor, these variations are comparable in magnitude to the absolute g -factor value. Therefore, the hole spin dephasing time $T_{2,h}^* \sim 0.25$ ns is quite fast, compared with the electron spin dephasing time of $T_{2,e}^* \sim 1.0$ ns.

At negative delays, before pump pulse arrival, a rephasing of the resident hole spins due to the SML effect is visible. This rephasing arises from spins whose precession about the magnetic field becomes synchronized with the laser-pulse repetition rate as expressed by the phase synchronization condition (PSC),⁷

$$\omega = \frac{|g_h| \mu_B B}{\hbar} = N \frac{2\pi}{T_R}, \quad (1)$$

where ω is the Larmor precession frequency determined by the hole g factor g_h along the magnetic field B , μ_B is the Bohr magneton, and N is a positive integer. Note, however, that the hole spin-mode-locking amplitude is weaker by a factor of 3 compared to the amplitude at positive delays as a result of the rather weak hyperfine interaction: The coupling to the nuclei, if efficient, would drive modes which do not initially fulfill the PSC into spin mode locking. This nuclear frequency focusing would occur by building up a nuclear field of proper strength that adds to the external magnetic field. Although being efficient for electrons, for which, after sufficiently long pumping, all optically excited ones can contribute to mode locking,¹⁵ the hyperfine interaction for holes is too weak to induce such nuclear frequency focusing.³ As a consequence, the negative delay signal is considerably weaker than the one at positive delays where the signal strength is determined by the entirety of excited dots.

For spin-echo experiments, an additional pulse, termed the control pulse, is introduced into the excitation scheme. This pulse is taken from a second Ti:sapphire laser system synchronized with the first one with a 100-fs accuracy but independently tunable in photon energy. Pulse duration and spectral width are equal for the two lasers. The second laser is used to rotate the hole spins about the optical z axis in analogy

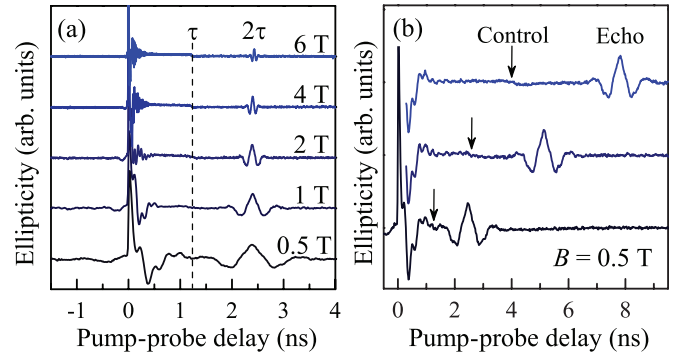


FIG. 2. (Color online) (a) Hole spin echoes at different magnetic fields. $\tau = 1.2$ ns and $T = 6$ K. Curves are shifted vertically for clarity. (b) Hole spin echoes for different control pulse delays $\tau = 1.2, 2.6,$ and 3.9 ns. The echo appearance time 2τ shifts in accordance with the control pulse arrival time τ . $B = 0.5$ T and $T = 6$ K.

to experiments on electron spin rotations in (In,Ga)As/GaAs QDs.¹⁶ The control pulse intensity is adjusted to a pulse area of 2π in order not to populate trion states, but to remain in the spin subspace of resident holes.

By adjusting the control photon energy to the pump photon energy, each control pulse rotates the resident hole spins in those QDs excited by the pump pulse by an angle of π . Figure 2(a) shows spin-rotation measurements at different magnetic fields varied from 0.5 to 6 T. The control pulse hits the sample at a time delay of $\tau = 1.2$ ns relative to the pump pulse arrival and at a time $2\tau = 2.4$ ns a hole spin echo appears. It arises from the 180° rotation of the hole spin ensemble at delay τ by which the dephasing, occurring between pump and control, is inverted and the spins reconvene. The temporal sequence is confirmed when the control pulse delay τ is varied as seen in Fig. 2(b). The time between echo formation and pump arrival is twice the time between control and pump.

The two effects, spin mode locking and spin echo, are exploited to determine the temperature dependence of the hole spin-coherence time. First, we turn to the spin-mode-locking signal in pure pump-probe studies without control pulses. Corresponding ellipticity traces are shown in Fig. 3(a) with a focus on the mode-locking signal at negative delay times, recorded for different temperatures. The pump pulse separation was 13.2 ns. Two contributions with different frequencies are seen in the signal; the one with the lower frequency is related to the hole spin precession of interest here. Because of the strong damping, even at the lowest temperatures, only one full oscillation is seen. The higher-frequency contribution can be assigned to the electron spin.

Clear hole SML can be seen in Fig. 3(a) up to temperatures of 15 K. From these observations, one identifies two temperature ranges for which we have to employ different methods for extracting the hole spin-coherence time T_2 . At the lower end of the studied temperatures ($T \lesssim 10$ K), T_2 is longer than the pulse repetition period T_R of 13.2 ns such that SML can occur. The appropriate method then is to increase T_R until the SML becomes weaker. From the variation in the SML amplitude with T_R , the spin-coherence time can be extracted.^{3,7} In contrast, if T_2 is shorter than T_R , as apparently is the case

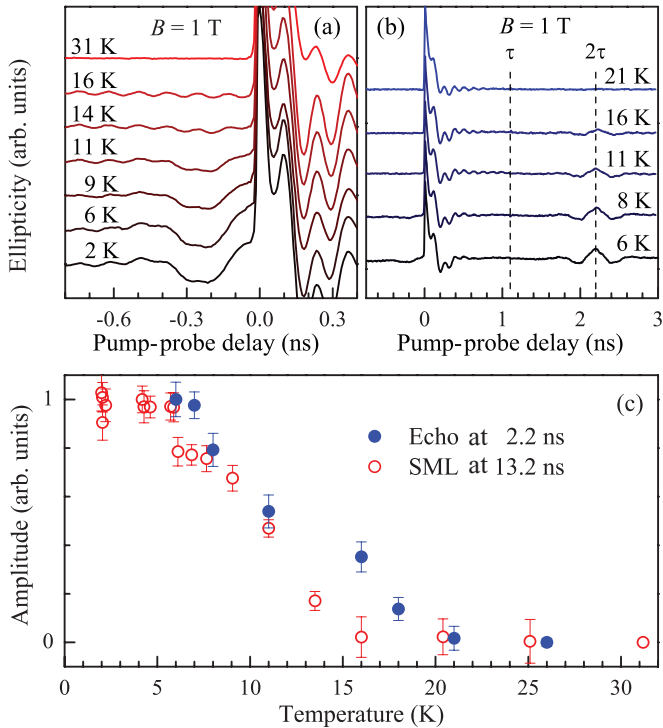


FIG. 3. (Color online) (a) Time-resolved ellipticity measurements with a focus on negative delay times for different temperatures; $B = 1$ T and $T_R = 13.2$ ns. Fits to the hole spin oscillations (see text) provide the SML amplitudes (red open circles) in panel (c). (b) Hole spin echoes recorded at different temperatures for $B = 1$ T, $T_R = 13.2$ ns, and $\tau = 1.1$ ns. From the echo oscillations, we deduce the blue data points (solid circles) in panel (c). (c) Temperature dependence of the normalized hole spin-echo (blue solid circles) and SML (red open circles) amplitudes.

for elevated temperatures, we can estimate the spin-coherence time from the temperature dependence of the SML amplitude and the spin-echo amplitude (see below).

Let us first concentrate on the low-temperature regime. To vary T_R , we implemented a pulse picker in the setup, which reduced the pulse repetition rate by letting only particular pulses of the original train pass while dumping the others. In that way, we increased the time between two subsequent pump pulses incrementally from $T_R = 132$ up to 660 ns and extracted the spin-mode-locking amplitude A_{SML} using a cosine fit with a Gaussian damping function. One can then determine the dependence of this amplitude on T_R and can obtain the coherence time T_2 using the following relation:

$$A_{\text{SML}}(T_R) \propto \exp \left[- \left(2 + \frac{1}{2\sqrt{3} + 3} \right) \frac{T_R}{T_2} \right], \quad (2)$$

which was derived in the supporting online material of Ref. 7. This is shown for two example temperatures in Fig. 4. The results for T_2 in dependence on the temperature are shown in Fig. 5 by filled circles. The hole spin-coherence time is constant at slightly more than $1 \mu\text{s}$ up to almost 6 to 7 K but then drops to about 100 ns at 10 K. A further temperature increase makes the SML disappear already for a pulse separation of 132 ns, which was the shortest that could technically be achieved with the pulse picker.

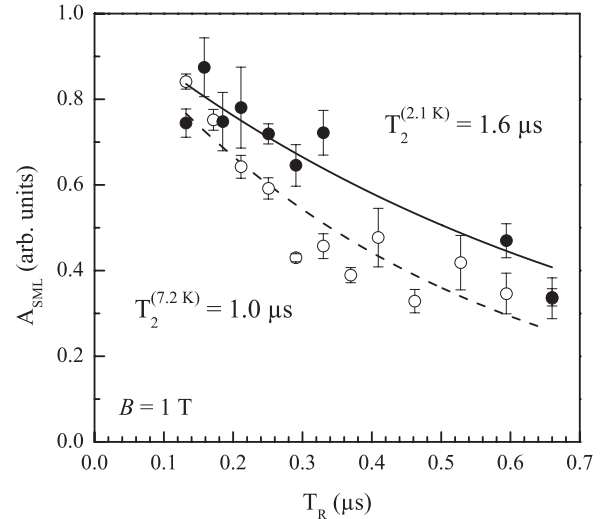


FIG. 4. Hole spin-mode-locking amplitudes A_{SML} depending on the repetition period T_R for two temperatures $T = 2.1$ K (solid circles) and $T = 7.2$ K (open circles); $B = 1$ T. Fits using Eq. (2) provide the respective coherence times $T_2^{(2.1 \text{ K})} = (1.6 \pm 0.3) \mu\text{s}$ and $T_2^{(7.2 \text{ K})} = (1.0 \pm 0.2) \mu\text{s}$.

In the elevated temperature range of $T > 10$ K, the other methods need to be applied, directly exploiting the temperature dependencies of spectroscopic quantities, such as the SML amplitude. Although this procedure is straightforward, only estimates for T_2 can be obtained in this way. Again, using a Gaussian-damped cosine fit, the amplitudes of the mode-locked resident hole spin polarization in Fig. 3(a) can be extracted. These amplitudes are plotted in Fig. 3(c). The drop in the amplitude between 5 and 15 K occurs because the spin-coherence time has become comparable to or shorter than the pulse separation of 13.2 ns. From the SML amplitudes before and after the drop as seen in Fig. 3(c), one can estimate that the hole spin-coherence time has to be around 7 ns at 15 K. The corresponding data point is inscribed in Fig. 5 by the vertically halved circle.

Another data point can be obtained from the temperature dependence of the hole spin-echo signal. In these studies, the control pulse hits the dephased hole spin ensemble at a 1.1-ns delay, leading to an echo at 2.2 ns as seen in Fig. 3(b). Similarly to the SML signal, the echo amplitude is constant at low temperatures but starts to decrease strongly at around 8 K and vanishes around 20 K. For analysis, the signal around the echo is also fitted by a cosine function with a Gaussian amplitude envelope. This amplitude is plotted in Fig. 3(c), being similar to the corresponding dependence for the SML signal. From this dependence, we get a data point of $T_2 = 1$ ns at $T = 20$ K.

Figure 5 shows the temperature dependence of the hole spin-coherence time and, for comparison, the electron spin-coherence time in a similar quantum dot sample published in Ref. 17. Electron and hole spin-coherence times are constant at low temperatures but then quickly decrease into the nanosecond range at moderate temperatures. Whereas, for the holes, this decrease is very abrupt and starts at 8 K, for the electrons, T_2 is constant in the microsecond range up to slightly more than 15 K before the drop occurs over a 30-K

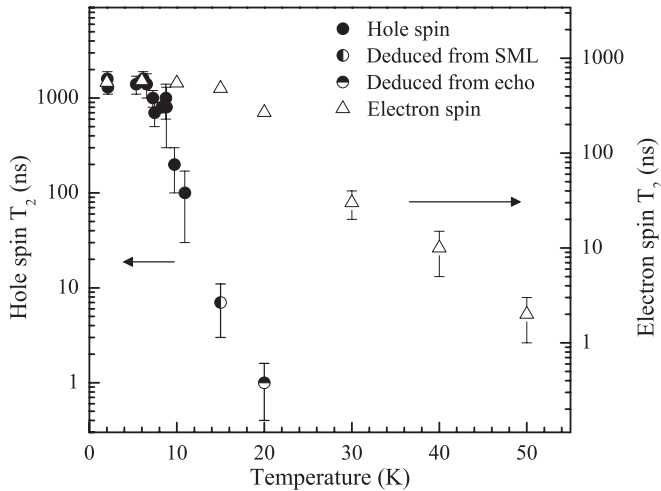


FIG. 5. Temperature dependence of the coherence time T_2 for hole spins (circles, left scale) and electron spins (triangles, right scale). The filled circles are measured by mode-locking experiments with various pulse separations at different temperatures (see text); $B = 1$ T. The vertically halved circle is deduced from the temperature dependence of the mode-locked spin amplitude with $T_R = 13.2$ ns; see Figs. 3(a) and 3(c). The horizontally halved circle is deduced from the temperature dependence of the hole spin echo; see Figs. 3(b) and 3(c). The electron data are taken from Ref. 17, being measured at $B = 2$ T. They are valid for comparison as, from 1 T up to 3 T, no magnetic-field dependence was observed.

range. For the electrons, the drop was associated with elastic scattering due to phonon-mediated fluctuations in the hyperfine interaction.¹⁷

Both the limitation of the hole spin coherence below a temperature of 8 K and the drop in coherence for higher temperatures need to be explained. Carrier spin coherence in quantum dots has been considered in a few papers in which either hyperfine interactions or spin-orbit-related interactions have been addressed as sources for decoherence. Let us first discuss the papers involving the nuclear bath: In the original paper by Fischer *et al.*,¹⁸ it was shown that, although the contact interaction is not relevant for holes, other contributions, the dipole-dipole interaction and the orbital angular momentum interaction with nuclear spins, can become important and may even be of comparable strength as the electron contact hyperfine interaction. Indications to that end were reported in Ref. 19.

It was recently demonstrated, however, that the hyperfine interaction is at least an order of magnitude weaker for holes than it is for electrons in self-assembled (In,Ga)As QDs.^{1-3,9,10,20,21} Based on these results, it is not evident that the interaction with the nuclei leads to the microsecond limit for the hole spin-coherence time. As mentioned, for the temperature dependence of the electron spin coherence, a model was also developed based on the spectral diffusion of the nuclear spin distribution due to excitation of acoustic phonons, which gives a good description of the experiment.^{17,22} Although it works well for electrons, due to the reduced nuclear interaction strength, this mechanism is unlikely to explain the temperature-induced drop in the hole spin coherence.

If we disregard the hole spin interaction with the nuclear spins, the spin-orbit interaction must account for the observed behavior of the hole spin-coherence time T_2 , involving phonon-mediated transitions between carrier spin levels. Corresponding transitions were already studied with respect to their impact on the longitudinal spin relaxation described by the T_1 time. For example, the spin-orbit-mediated single-phonon scattering was used to describe the hole spin relaxation in (In,Ga)As QDs, giving T_1 times of up to 270 μ s.²³ Furthermore, two-phonon-assisted spin relaxation was considered theoretically for hole spins, giving T_1 times of hundreds of microseconds in finite magnetic fields, in particular, at $B = 2$ T and $T = 2$ K as in the experiment here.^{24,25} However, recent experimental studies of InAs QDs demonstrated comparatively short longitudinal relaxation times of $T_1 = 2.4$ μ s at $B = 2$ T,²⁶ suggesting a much stronger spin-orbit coupling than previously assumed.

When considering transverse spin relaxation, a spin might become excited without a spin flip through phonon absorption to an excited orbital state having a different g factor, resulting in a different precession frequency. After relaxation, this would lead to a phase change in the spin precession.²² In addition, the impact of anharmonic phonons due to lattice impurities, defects, etc., has been acknowledged. Interactions with them can also lead to a phase change in the coherent spin dynamics.²² These mechanisms formulated for electrons are obviously also relevant for holes, potentially even more prominently as the spin-orbit interaction is stronger in the valence band. The vacuum phonon fields enable these interactions but would not, however, contribute to their thermal activation.

The mechanism based on the g -factor variation requires excitation of a hole from the ground to an excited state. From the splitting of about 20 meV between the first-excited-state and the ground-state emission (obtained from high-excitation photoluminescence studies), we estimate a splitting of the corresponding valence-band states of at least 5 meV,²⁷ whereas, the temperature of 8 K, at which the sharp drop in T_2 sets in, is considerably less than 1 meV.²⁸ This makes such an excitation very unlikely. If the other mechanisms also rely on processes, such as two-phonon scattering into an excited state and back down to the ground level, they also cannot explain the observed strong temperature dependence of elastic spin scattering. We also note that crystal defects in self-assembled QDs have been shown to be strongly suppressed as also evidenced by the high optical quality of the studied structures.

We suggest, therefore, a different mechanism. For quantum dots, the interaction of carriers with acoustic phonons has been shown to have important consequences. For example, due to it, the coherent exciton polarization drops over a time scale of a few picoseconds after pulsed carrier excitation, limiting the quantum-mechanical coherence.²⁹ In the spectral domain, this scattering results in broad spectral flanks of the zero-phonon spectral line of the QD exciton transition.^{30,31} The underlying mechanism can be understood as follows: The carriers lead to the formation of a quasistable polaron, a bound state of the injected charges, and an associated phonon population by which the lattice becomes distorted. As a result of this distortion, a coherent phonon wave packet is emitted from the QDs, escaping on time scales of picoseconds into the embedding material.

The coupling to acoustic phonons is also important for the radiative decay of exciton complexes. In QDs embedded in an optical resonator, not only excitons, whose energy coincides with a resonator mode, can decay. Through the phonon sidebands, QDs whose transition energy is off-resonant can also radiate into the mode. In that way, the laser threshold is reduced, and the laser output is increased.^{32–36}

Due to the significance of the coupling of QD charges with acoustic phonons, we suggest that it also enables elastic two-phonon scattering, leading to a destruction of the phase coherence of the hole spin. Since the phonon sidebands offer a continuum of multiple interaction options, these two phonon processes may, in sum, become efficient. The resulting elastic scattering of the hole spin may explain the restriction of the hole spin-coherence time to microseconds below 8 K and might also explain the speedup of spin relaxation at moderate temperatures around 10 K, at which acoustic phonon modes lying within the phonon sidebands become thermally

activated. However, still more detailed studies need to be performed.

To summarize, we have studied the temperature dependence of the hole spin-coherence time T_2 by making use of the spin-mode-locking effect and all-optically-created hole spin echoes. The sharp drop in T_2 from microseconds down to nanoseconds below 20 K suggests that mechanisms considered so far, based on the hyperfine coupling and the spin-orbit interaction, are not adequate for explanation and that further considerations may be required. Here, we have suggested an alternative mechanism relying on elastic scattering exploiting the broad phonon sidebands. Perspectives for the further coherent manipulation of hole spins include multiecho techniques, which might be used in dynamic decoupling schemes by which the spin-coherence time might be extended, as in NMR experiments.³⁷

This work was supported by the Deutsche Forschungsgemeinschaft and the BMBF project QuaHL-Rep.

-
- ¹P. Fallahi, S. T. Yilmaz, and A. Imamoglu, *Phys. Rev. Lett.* **105**, 257402 (2010).
- ²E. A. Chekhovich, A. B. Krysa, M. S. Skolnick, and A. I. Tartakovskii, *Phys. Rev. Lett.* **106**, 027402 (2011).
- ³S. Varwig, A. Schwan, D. Barmascheid, C. Müller, A. Greilich, I. A. Yugova, D. R. Yakovlev, D. Reuter, A. D. Wieck, and M. Bayer, *Phys. Rev. B* **86**, 075321 (2012).
- ⁴I. A. Merkulov, A. L. Efros, and M. Rosen, *Phys. Rev. B* **65**, 205309 (2002).
- ⁵A. V. Khaetskii, D. Loss, and L. Glazman, *Phys. Rev. Lett.* **88**, 186802 (2002).
- ⁶J. R. Petta, A. C. Johnson, J. M. Taylor, E. A. Laird, A. Yacoby, M. D. Lukin, C. M. Marcus, M. P. Hanson, and A. C. Gossard, *Science* **309**, 2180 (2005).
- ⁷A. Greilich, D. R. Yakovlev, A. Shabaev, A. L. Efros, I. A. Yugova, R. Oulton, V. Stavarache, D. Reuter, A. D. Wieck, and M. Bayer, *Science* **313**, 341 (2006).
- ⁸J. Fischer and D. Loss, *Phys. Rev. Lett.* **105**, 266603 (2010).
- ⁹K. De Greve, P. L. McMahon, D. Press, T. D. Ladd, D. Bisping, C. Schneider, M. Kamp, L. Worschech, S. Höfling, A. Forchel, and Y. Yamamoto, *Nat. Phys.* **7**, 872 (2011).
- ¹⁰F. Fras, B. Eble, B. Siarry, F. Bernardot, A. Miard, A. Lemaître, C. Testelin, and M. Chamarro, *Phys. Rev. B* **86**, 161303(R) (2012).
- ¹¹R. Dabashi, J. Hübner, F. Berski, J. Wiegand, X. Marie, K. Pierz, H. W. Schumacher, and M. Oestreich, *Appl. Phys. Lett.* **100**, 031906 (2012).
- ¹²Y. Li, N. Sinitsyn, D. L. Smith, D. Reuter, A. D. Wieck, D. R. Yakovlev, M. Bayer, and S. A. Crooker, *Phys. Rev. Lett.* **108**, 186603 (2012).
- ¹³This value was determined with an accuracy of ± 0.02 from the hole spin echoes described below, coinciding with the g -factor analysis of the same sample in Ref. 3.
- ¹⁴I. A. Yugova, A. Greilich, E. A. Zhukov, D. R. Yakovlev, M. Bayer, D. Reuter, and A. D. Wieck, *Phys. Rev. B* **75**, 195325 (2007).
- ¹⁵A. Greilich, A. Shabaev, D. R. Yakovlev, A. L. Efros, I. A. Yugova, D. Reuter, A. D. Wieck, and M. Bayer, *Science* **317**, 1896 (2007).
- ¹⁶A. Greilich, S. E. Economou, S. Spatzek, D. R. Yakovlev, D. Reuter, A. D. Wieck, T. L. Reinecke, and M. Bayer, *Nat. Phys.* **5**, 262 (2009).
- ¹⁷F. G. G. Hernandez, A. Greilich, F. Brito, M. Wiemann, D. R. Yakovlev, D. Reuter, A. D. Wieck, and M. Bayer, *Phys. Rev. B* **78**, 041303(R) (2008).
- ¹⁸J. Fischer, W. A. Coish, D. V. Bulaev, and D. Loss, *Phys. Rev. B* **78**, 155329 (2008).
- ¹⁹C. Testelin, F. Bernardot, B. Eble, and M. Chamarro, *Phys. Rev. B* **79**, 195440 (2009).
- ²⁰B. Eble, C. Testelin, P. Desfonds, F. Bernardot, A. Balocchi, T. Amand, A. Miard, A. Lemaître, X. Marie, and M. Chamarro, *Phys. Rev. Lett.* **102**, 146601 (2009).
- ²¹X. J. Wang, S. Chesi, and W. A. Coish, *Phys. Rev. Lett.* **109**, 237601 (2012).
- ²²Y. G. Semenov and K. W. Kim, *Phys. Rev. B* **75**, 195342 (2007).
- ²³D. Heiss, S. Schaeck, H. Huebl, M. Bichler, G. Abstreiter, J. J. Finley, D. V. Bulaev, and D. Loss, *Phys. Rev. B* **76**, 241306(R) (2007).
- ²⁴M. Trif, P. Simon, and D. Loss, *Phys. Rev. Lett.* **103**, 106601 (2009).
- ²⁵C. Lü, J. L. Cheng, and M. W. Wu, *Phys. Rev. B* **71**, 075308 (2005).
- ²⁶F. Fras, B. Eble, P. Desfonds, F. Bernardot, C. Testelin, M. Chamarro, A. Miard, and A. Lemaître, *Phys. Rev. B* **86**, 045306 (2012).
- ²⁷E. A. Zibik, A. D. Andreev, L. R. Wilson, M. J. Steer, R. P. Green, W. H. Ng, J. W. Cockburn, M. S. Skolnick, and M. Hopkinson, *Physica E (Amsterdam)* **26**, 105 (2005).
- ²⁸We note that thermal escape of carriers out of the QD confinement potential does not play a role in the studied temperature range as confirmed by a constant ground-state emission intensity.
- ²⁹E. Tsitsishvili, R. v. Baltz, and H. Kalt, *Phys. Rev. B* **66**, 161405(R) (2002).
- ³⁰P. Borri, W. Langbein, S. Schneider, U. Woggon, R. L. Sellin, D. Ouyang, and D. Bimberg, *Phys. Rev. Lett.* **87**, 157401 (2001).
- ³¹A. Vagov, V. M. Axt, and T. Kuhn, *Phys. Rev. B* **66**, 165312 (2002).

- ³²M. Kaniber, A. Laucht, A. Neumann, J. M. Villas-Bôas, M. Bichler, M.-C. Amann, and J. J. Finley, *Phys. Rev. B* **77**, 161303(R) (2008).
- ³³D. Press, S. Götzinger, S. Reitzenstein, C. Hofmann, A. Löffler, M. Kamp, A. Forchel, and Y. Yamamoto, *Phys. Rev. Lett.* **98**, 117402 (2007).
- ³⁴K. Hennessy, A. Badolato, M. Winger, D. Gerace, M. Atatüre, S. Gulde, S. Fält, E. L. Hu, and A. Imamoglu, *Nature (London)* **445**, 896 (2007).
- ³⁵M. Winger, T. Volz, G. Tarel, S. Portolan, A. Badolato, K. J. Hennessy, E. L. Hu, A. Beveratos, J. Finley, V. Savona, and A. Imamoglu, *Phys. Rev. Lett.* **103**, 207403 (2009).
- ³⁶S. Ates, S. M. Ulrich, A. Ulhaq, S. Reitzenstein, A. Löffler, S. Höfling, A. Forchel, and P. Michler, *Nat. Photonics* **3**, 724 (2009).
- ³⁷H. Bluhm, S. Foletti, I. Neder, M. Rudner, D. Mahalu, V. Umansky, and A. Yacoby, *Nat. Phys.* **7**, 109 (2011).